ELSEVIER

Polymer 42 (2001) 5643–5650

polymer

www.elsevier.nl/locate/polymer

Effect of moisture on the tensile properties of poly(hydroxy ester ether)☆

S. St. Lawrence[a], J.L. Willett[a,*], C.J. Carriere[b]

[a] *Plant Polymer Research Unit, National Center for Agricultural Utilization Research, USDA-ARS, 1815 N. University St., Peoria, IL 61604, USA*
[b] *Biomaterials Processing Research, National Center for Agricultural Utilization Research, USDA-ARS, 1815 N. University St., Peoria, IL 61604, USA*

Received 14 August 2000; received in revised form 8 November 2000; accepted 9 November 2000

Abstract

The effects of moisture and strain rate on the tensile properties of poly(hydroxy ester ether) (PHEE) were investigated. Water was shown to act as a plasticiser which lowered the room temperature tensile strength and modulus. The strain at failure increased with increasing water content and a change in the mode of failure was observed. Brittle failure occurred when the moisture content was low. As the sorbed water content increased, the samples necked and extensive plastic deformation resulted. The samples deformed in a quasi-homogeneous manner at testing temperatures close to the glass transition temperature. The yield stress decreased with moisture content and increased with strain rate. For samples which deformed in a ductile manner, the variation in the yield stress with strain rate was well described using the Eyring model. The effect of water content on the yield stress was shown to be analogous to the effect of temperature. © 2001 Published by Elsevier Science Ltd.

Keywords: Poly(hydroxy ester ether); Moisture content; Tensile properties

1. Introduction

Disposal of oil-based polymers creates a waste management problem due to their low density and high production volume [1]. This problem can be reduced to some extent by recycling and energy recovery programs. However, the unique properties of biodegradable polymers provide certain advantages not offered by these other alternates. First, polymers made from renewable sources will reduce the demand for petroleum products [1]. Second, biodegradable and bio-compatible polymers are ideally suited for use in the pharmaceutical industry both as packaging materials and for surgical fixation [1,2]. Third, composting biodegradable polymers will help to meet the anticipated demand for biomass needed for agricultural applications [3].

Despite their appealing properties, biodegradable polymers have not been commercially successful except in some niche markets [1]. The chief hindrance to more wide scale use is their prohibitively high cost. In an effort to reduce the cost, these materials have been blended with lower cost polymers or alternatively an inexpensive filler has been added. Starch, in its native granule form, has been studied as a possible filler and, following gelatination, it has been blended with biodegradable polymers [4–12]. Typically, the addition of starch reduces the strength and elongation at failure but improves degradation rates. The reduction in mechanical properties is generally attributed to the poor adhesion between starch and most polymers [4]. A recently developed biodegradable thermoplastic epoxy (PHEE), however, has been shown to have improved adhesion and as a result, composites of these materials have mechanical properties that are comparable to commercial grade polystyrene although they are susceptible to water damage [5–7].

Absorbed moisture affects the fracture toughness, the tensile properties and the viscoelastic behaviour of some polymers [13–17]. These mechanical properties are altered if the sorbed moisture: (1) introduces swelling stresses, (2) interacts with other environmental factors, (3) changes the mode of failure, and (4) acts as a plasticiser which lowers the glass transition temperature, T_g. In the latter case, the effect of the moisture content has been shown to be analogous to the effect of temperature and can be described using similar mathematical functions [14]. Emri and Pavsek [14] created a master curve of the shear compliance by shifting

☆ Names are necessary to report factually on available data: however, the USDA neither guarantees nor warrants the standard of the product and the use of the nane by the USDA implies no approval of the product to the exclusion of others that may also be suitable.

* Corresponding author. Tel.: +1-309-681-6556; fax: +1-309-681-6691.
E-mail addresses: stlawrs@mail.ncaur.usda.gov (S. St. Lawrence), willetjl@mail.ncaur.usda.gov (J.L. Willett).

0032-3861/01/$ - see front matter © 2001 Published by Elsevier Science Ltd.
PII: S0032-3861(00)00836-3

data from different moisture levels to a common reference point using an equation of the same form as the well known WLF equation [18].

It has been shown that water acts as a plasticiser for PHEE and lowers the T_g from approximately 40°C when dry to ~4°C when the water content is maximum, ~5.8 wt% [7]. Although the drop in T_g is small compared to starch, it dramatically alters the room temperature mechanical properties. In order to understand the response of this polymer to a given loading condition, the effect of moisture content on the mechanical properties must be determined. This is particularly important if the polymer is to be blended or if a low cost filler is added. The purpose of the present work is to investigate the changes in the mechanical properties of PHEE with moisture content. The equivalence between moisture content and temperature was examined and the Eyring theory was used to model the yield stress behaviour.

2. Experimental

The PHEE studied in this investigation, belongs to a group of polymers that are produced by a reaction of diacids with an equivalent amount of diglycidyl ethers where quaternary ammonium salts are used as initiators to avoid crosslinking and transesterification [19,20]. This particular PHEE, is derived from the diglycidyl ether of bisphenol A and adipic acid. It is an amorphous polymer with a glass transition temperature of approximately 40°C when dry (measured by differential scanning calorimetry) and after compression moulding, $M_w = 9.1 \times 10^4$(g/mol) (determined by light scattering) [21].

Samples for tensile tests and for dynamic mechanical analysis (DMA) were cut from compression moulded thin sheets of thickness ~1 mm. The pellets were dried before compression moulding to eliminate air holes. The sheets were slowly cooled from a moulding temperature of 120°C to room temperature, at approximately 0.5 °C/min, to reduce internal stresses. The dogbone shaped tensile bars had a gauge length of 25 mm and a width of 4 mm. Samples for the DMA analysis were ~2 mm wide. To vary the moisture content, the compression moulded sheets were conditioned in environmental chambers of different relativity humidity; 10, 30, 50 and 70%. The sheets were held in the chambers for approximately 30 days to ensure that the moisture content was constant across the thickness. Compression moulded sheets were also dried for a further 14 days to lower the water content. The water content was measured using a Mettler Toledo model LJ16 moisture analyser.

All tension tests were performed on an Instron model 4201 Universal Testing Frame operated using Series IX software. The crosshead speed was varied from 0.5 to 300 mm/min which corresponds to strain rates between 3.3×10^{-4} and $0.2\ s^{-1}$. Engineering strain, ϵ, was determined by measuring the displacement of bench marks on the gauge length using a digital video camera. This method was only accurate at large strains where the error in the measurement was small compared with the actual displacements. At small strains the relative error was larger and it was not possible to maintain an acceptable level of accuracy. The engineering stress, σ was defined as the load, P divided by the initial cross section area, A_0. Young's modulus, E (σ/ϵ) was calculated using the displacement measured by the Instron. Due to the error in the strain measurement, the modulus was only used for comparative purposes. The yield stress, σ_y, was defined either as the point were the load passed through a local maximum or at the intersection of two lines drawn parallel to the $\sigma-\epsilon$ curve at small strains. The tests were performed at 50% relative humidity and at 22.7 ± 0.6°C unless noted otherwise. For higher temperatures a furnace was attached to the testing frame. A minimum of three samples were tested at each condition.

The glass transition temperature, T_g, was determined using a Perkin–Elmer DMA 7. The samples were tested in tension at an excitation frequency of 1 Hz and a heating rate of 1 °C/min. The samples were scanned from approximately 5 to 50°C. The T_g was taken as the loss modulus, E'' peak.

Fracture surfaces were examined using either a JEOL scanning electron microscope or a Zeiss stereo optical microscope. Samples for SEM were sputter coated with a thin layer of gold/palladium and examined using a low beam voltage (2–5 kV) to prevent damaging the fracture surface.

3. Results

3.1. Glass transition temperature

For the samples conditioned in environments of different relative humidity (r.h.) the glass transition temperature, moisture content and the degree of undercooling, ΔT, are given in Table 1. Here, ΔT is defined as the temperature

Table 1
Glass transition temperature and water content of PHEE samples conditions in atmospheres with different relative humidity

Relative humidity	Water content (%)	Glass transition temperature, T_g (°C)	Degree of undercooling, ΔT[a] (°C)
0	0.29	37.1 ± 0.9	−14
10	0.53	34.6 ± 0.6	−12.5
30	0.93	29.9 ± 0.5	−6.5
50	1.33	24.9 ± 0.5	−3
70(1)	1.73	21.5 ± 0.7	0.5
70(2)[b]	1.73	21.5 ± 0.7	4

[a] The degree of undercooling is given by $\Delta T = T_i - T_g$ where, T_i is the testing temperature.
[b] Samples conditioned at 70% r.h. and tested at 25.5°C.

difference between the testing temperature, T_i and the measured T_g. As expected the dried material has the highest T_g (37°C) and the largest negative ΔT (−14°C).

As the r.h. and subsequently the moisture content increase both the T_g and the magnitude of ΔT decrease. For samples conditioned at the highest r.h. (70%) the glass transition temperature is approximately equal to the testing temperature ($\Delta T = +0.5$). Material conditioned at this relative humidity was also tested at a higher temperature, ($\Delta T = +4$°C).

3.2. Tensile properties

The tensile strength, σ_u, Young's modulus, E and strain at failure, ϵ_f are shown in Fig. 1 as a function of the degree of undercooling for three strain rates, $\dot{\epsilon}$. The data are presented in this manner to illustrate the strong influence that ΔT and consequently, the moisture content, have on the mechanical properties of PHEE. For each $\dot{\epsilon}$ the entire range of ΔT is not covered because the tests were performed at specific strain rates depending on the behaviour of the material. The lines through the data points in Fig. 1 are only included as visual aids to highlight trends.

Both the degree of undercooling and the strain rate affect the tensile strength of PHEE. However, of the two the influence of ΔT is more significant (Fig. 1a). The strength increases as the degree of undercooling increases or as the moisture content decreases. At large negative ΔT, σ_u is between 50 and 65 MPa and drops to less than 5 MPa at $\Delta T = +4$°C for all three strain rates. This behaviour is analogous to the effect of increasing temperature on the tensile strength of glassy polymers [22]. In general, as the temperature approaches T_g there is a decrease in both the tensile strength and the yield stress. The tensile strength of PHEE is also affected by $\dot{\epsilon}$. For example, at a ΔT value of +4°C or −6.5°C, σ_u doubles as the strain rate increases from 0.03 to 0.2 s^{-1}. However, when $\Delta T = -14$°C, σ_u is largely independent of $\dot{\epsilon}$ above 0.03 s^{-1}. At these testing rates, the samples fail in a brittle manner and the tensile strength is approximately 63 MPa. The increased strength and brittleness are an indication of reduced chain mobility as the degree of undercooling increases.

The effect of moisture content, as reflected in the change in T_g, on Young's modulus of PHEE is analogous to the normally encountered dependence on temperature [23]. At temperatures well below T_g, the modulus of an amorphous polymer is essentially constant showing only a small dependence on temperature and testing rate since the molecules are immobilised. Large changes in viscoelastic properties, such as E, are absent. This behaviour is true of PHEE when $\Delta T \geq -12.5$°C as shown in Fig. 1b. At temperatures closer to T_g, in the transition region, the modulus of an amorphous polymer is very changeable. For PHEE the modulus decreases by two orders of magnitude between $\Delta T = -12.5$ and ~0°C. The effect of $\dot{\epsilon}$ on the modulus is also most pronounced at intermediate ΔT (from −10 to +0.5°C). Above T_g, in the rubbery state, the modulus of an amorphous polymer is again constant since molecular mobility is considerably higher than the rate of change of the loading conditions. Again, this is the case for PHEE at $\Delta T = +4$°C. The changes in the modulus with moisture content are analogous to the effect of temperature. With increasing moisture, the mechanical properties of PHEE change from glassy to rubbery with an intermediate transitional stage.

The effect of strain rate and degree of undercooling on ϵ_f is shown in Fig. 1c. At large negative ΔT, failure tends to occur before the sample yields and $\epsilon_f < 10\%$ for all strain rates. At less negative ΔT (> − 12.5°C) failure occurs after the sample yields and ϵ_f increases rapidly as the degree of undercooling is reduced. Between $\Delta T = -12.5$ and ~0°C there is at least a four-fold increase in ϵ_f at strain rates of 3×10^{-3} and 0.03 s^{-1}. At the highest strain rate (0.2 s^{-1}) there is a similar increase in ϵ_f between $\Delta T = -6.5$ and +4°C. As expected, the largest strain at failure (>400%), occurs when the testing temperature is above T_g($\Delta T = +4$°C). The increase in ϵ_f is a result of the absorbed water which acts as a plasticiser. A similar behaviour has been reported for PMMA at low moisture levels [13]. However, for PMMA there is a decrease in ϵ_f at larger moisture contents which is attributed to the formation of water clusters that act as fillers [13]. If the sorbed moisture forms clusters in PHEE it does not result in a reduction in ϵ_f.

3.3. Changes in the fracture behaviour

The shape of the σ–ϵ curve changed significantly over the range of moisture content and therefore, ΔT studied. At large negative ΔT and high strain rates, failure occurs either before the sample yields or shortly after. In the latter case, the load does not drop to a constant plateau level after the yield point (Fig. 2, $\Delta T = -12.5$°C). Between $\Delta T = -6.5$ and −3°C, the σ–ϵ curve has a local load maximum at the yield point followed by strain softening. Closer to failure, there is a second drop in the load which is due to the growth of a fatal crack. At $\Delta T = +0.5$°C, there is an inflection point in the σ–ϵ curve at small strains but no strain softening. Strain hardening begins almost immediately following the yield point. In general, as ΔT approaches zero there is a reduction and eventual disappearance in strain softening as shown in the insert of Fig. 2. Finally, at a testing temperature above the T_g($\Delta T = +4$°C) the material behaves like a viscoelastic liquid. Under these conditions, there is no load maximum at the yield point only a gradual increase in the load with increasing strain. The stress eventually reaches a maximum before it begins to decrease due to crack growth.

The effect of strain rate on the shape of the σ–ϵ curve depends on the degree of undercooling. Close to the T_g ($\Delta T \sim 0$°C) the yield stress is strongly affected by the strain rate and there is a noticeable reduction in strain softening as $\dot{\epsilon}$ decreases. At larger negative ΔT, the effect of strain rate is

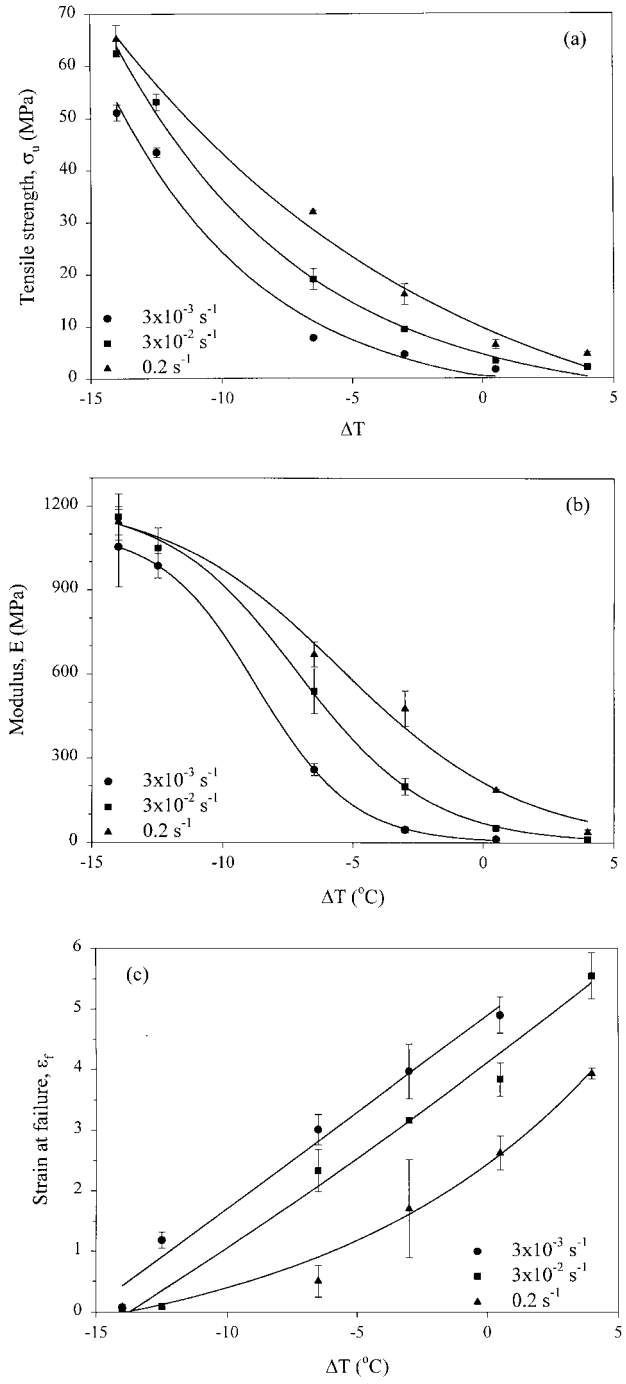

Fig. 1. Tensile properties versus ΔT for PHEE at strain rates of: (●) $3.3 \times 10^{-3}\,s^{-1}$, (■) $3.3 \times 10^{-2}\,s^{-1}$ and (▲) $0.2\,s^{-1}$. (a) Ultimate tensile strength, σ_u; (b) tensile modulus, E; and (c) strain at failure, ϵ_f.

less pronounced. A transition from brittle to ductile occurs as strain rate decreases but once yielding begins the overall shape of the $\sigma-\epsilon$ curve is similar. The strong dependence between the $\sigma-\epsilon$ behaviour and the strain rate at temperature close to T_g is similar to other amorphous polymers such as PC [24].

Three different modes of failure have been identified for PHEE as shown on the ΔT versus $\dot{\epsilon}$ graph in Fig. 3. Brittle failure occurs if the sample fractures before yielding. If the sample yields and strain softens the failure process is ductile but if there is no strain softening the failure mode is termed rubbery. Over the limited range of ΔT and strain rates investigated, PHEE displays all three modes of failure. Ductile behaviour is confined to a narrow range of ΔT, between approximately 0 and -15°C. This region is bonded by the ductile–brittle transition in the lower right-hand corner and by the rubbery–ductile transition in the upper left-hand corner. The range of ΔT over which PHEE displays ductile behaviour is smaller than for cross-linked epoxy [25].

Changes in the mode of failure are accompanied by changes in the appearance of the tensile bar during extension and the fracture surface after failure. Samples which fail in a ductile manner at large negative ΔT (-12.5°C) form a sharp neck with pronounced shoulders, see Fig. 4a. As the material displays more rubber-like behaviour the neck becomes shallower until at small enough ΔT or low enough strain rates, deformation becomes quasi-homogeneous as shown in Fig. 4b. The appearance of this sample is typical for samples tested at $\Delta T = +4$°C.

For samples that deform in a quasi-homogeneous manner the entire gauge length stress whitens before failure. This also occurs when a more distinct neck is formed and failure occurs at high extensions. At larger degrees of undercooling, the stress whitened region is small and centred around the eventual fracture site. Well-defined broad shear zones are evident above and below the fracture plane at $\Delta T = -12.5$°C for samples that yield before fracturing. Such zones are not seen when ΔT is above -10°C. At a testing temperature above T_g($\Delta T = +4$°C) numerous cracks form along the gauge length (Fig. 5). The appearance of these cracks always coincides with a drop in load at high strains.

The appearance of the fracture surface varied greatly with the degree of undercooling and the strain rate. At large negative ΔT and high $\dot{\epsilon}$ the fracture surface is typical of brittle failure (Fig. 6). The initiation site (lower left-hand side) is surrounded by a smooth featureless semi-circular zone. Away from the initiation site the rough surface is due to crack branching which is clearly visible prior to failure. At smaller degrees of undercooling the fracture surfaces are smoother and covered in fine striations which extend away from the initiation site (lower right-hand corner Fig. 7a). For both ductile and rubbery materials a smooth fracture surface is typical except at $\Delta T = +4$°C (Fig. 7b). Instead of fine striations, the fracture surface is covered in deep markings which are formed by the intersection of the primary crack with the secondary cracks. Cracks of different lengths are evident on the outer surface of samples tested at $\Delta T = +4$°C (Fig. 5). Both the number of cracks and the average length of the cracks increase as the testing speed decreases. The changes in the appearance of the fracture surface with ΔT or r.h. are similar to those shown previously for epoxies tested at different temperatures [26].

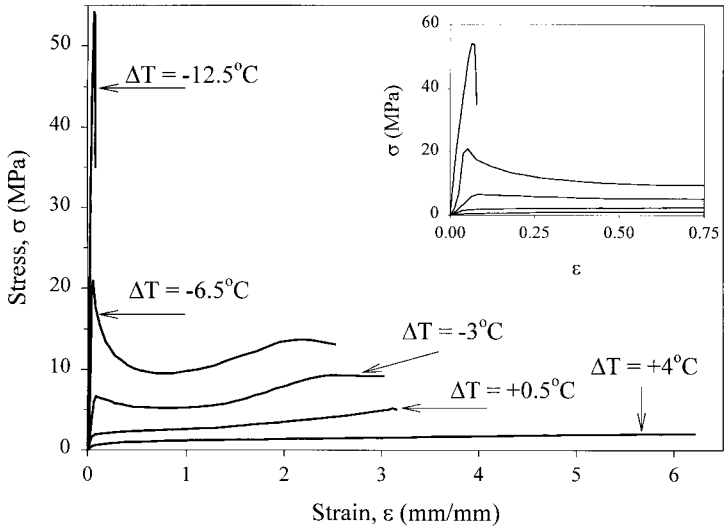

Fig. 2. Stress–strain curves for PHEE at different ΔT at a strain rate of $3.3 \times 10^{-2}\ s^{-1}$. The small strain region is shown in the insert.

3.4. Yielding behaviour

At degrees of undercooling between $\Delta T \approx 0$ and -14°C, the samples deform in a ductile manner with a load maximum at the yield point followed by strain softening. In the following section, this load maximum will be used to define the yield stress. For samples that do not exhibit strain softening, determining the yield stress is subjected to larger errors.

For many polymers the variation in yield stress, σ_y with temperature, T and strain rate, $\dot{\epsilon}$ can be described using the flow model of Eyring [27,28]. According to this theory, yielding occurs when segments of molecules possess sufficient energy to overcome a barrier to motion. An applied stress reduces this energy barrier and allows the molecular segments to move in the forward direction, i.e. in the direction of the applied stress. Movement in the reverse direction is negligible since it is assumed to occur slowly even prior to the application of the stress. The macroscopic strain is then assumed to be proportional to the rate at which segments move in the forward direction. The relationship between the tensile stress, σ and the strain rate is given by [28]:

$$\frac{\sigma}{T} = 2\left[\frac{\Delta H}{v} + 2.303\frac{R}{v}\log\left(\frac{\dot{\epsilon}}{\dot{\epsilon}_o}\right)\right] \quad (1)$$

where v is the activation volume, ΔH the activation energy, R the gas constant and $\dot{\epsilon}_o$ a constant.

The Eyring equation predicts a logarithmic relationship between the yield stress and the strain rate at a given temperature. For the present experiments, the testing temperature was held constant, but the degree of undercooling ΔT was changed due to differences in material's

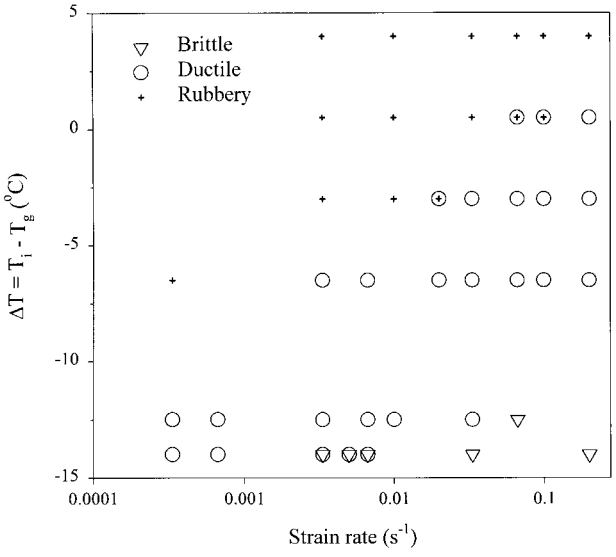

Fig. 3. Tensile failure modes for PHEE shown on a plot of ΔT versus $\dot{\epsilon}$. Overlaid symbols designate mixed modes of failure.

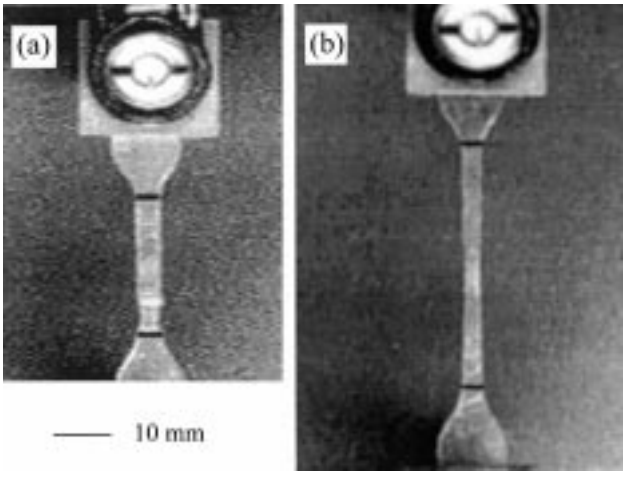

Fig. 4. Neck profiles photographed while the specimens were being drawn at: (a) $\Delta T = -14$°C and $\dot{\epsilon} = 3.3 \times 10^{-4}\ s^{-1}$; and (b) $\Delta T = -6.5$°C and $\dot{\epsilon} = 7.9 \times 10^{-2}\ s^{-1}$.

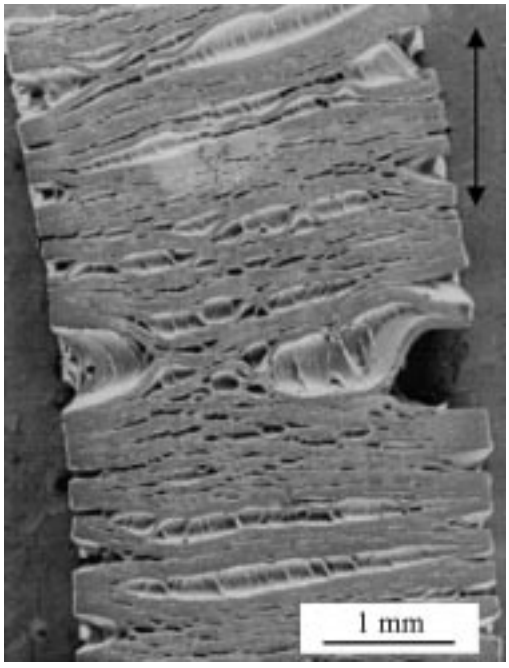

Fig. 5. Outer surfaces of a tensile sample following failure, ($\Delta T = +4$°C and $\dot{\epsilon} = 3.3 \times 10^{-4}\ s^{-1}$). The arrow indicates the direction of applied stress.

glass transition temperature (Table 1). To describe the effect of a change in T_g, T in Eq. (1) was replaced by T^* where, $T^* = T_r + \Delta T$ and T_r is a reference temperature (296 K). For materials conditioned at 70% r.h. $T^* \approx 296$ K and $T^* =$ 282 F for the dried material.

At strain rates and ΔT values where the material deforms in a ductile manner, plots of σ_y/T^* against $\log(\dot{\epsilon})$ give a series of parallel straight lines (Fig. 8) in agreement with the theory. The effect of moisture content on the T_g and the yield behaviour is analogous to the usual effect of temperature. In the ductile region, the activation volume at each T^* is approximately constant and equal to $1.5 \pm 0.17\ nm^3$. When the samples display rubbery behaviour, the yield stress increases more slowly with increasing $\dot{\epsilon}$. At the transition from rubbery to ductile behaviour, there is a distinct increase in the slope of the T^* versus $\log(\dot{\epsilon})$ curves with a corresponding decrease in v. At $T^* = 293$ K, the slope increases at a strain rate of $1.97 \times 10^{-2}\ s^{-1}$ and at $T^* \approx 296$ K the inflection point occurs at $3.28 \times 10^{-2}\ s^{-1}$. In the latter case, v is comparatively large even at strain rates where the samples display mixed ductile and rubbery behaviour. Above the transition point, the activation volume is $\sim 3.0\ nm^3$ which is twice v in the ductile region. The increase in v suggests that one activated rate process dominates at low $\dot{\epsilon}$ and small ΔT and the other at high strain rates and large ΔT. Similar changes in the slopes of σ_y/T against $\log(\dot{\epsilon})$ curves have been reported for PMMA, PVC and PC [29]. For these materials the yield behaviour was successfully explained using two activated rate processes.

For polymers the yield stress can be estimated at strain rates that are not accessible experimentally by creating a master curve. This curve is made by shifting experimental data from different temperatures to a common reference temperature in accordance with the time–temperature superposition principle [30]. A master curve can be made for PHEE, using the data from Fig. 8, if the data at each T^* is represented by the equation.

$$\sigma_y = C_1 + C_2 \log(\dot{\epsilon} a_t) \tag{2}$$

where C_1 and C_2 are constants and a_t the shift factor.

The master curve created using a reference $T^* = 289.5$ K is shown in Fig. 9. This T^* was chosen as the reference point because the samples display ductile behaviour over the broadest range of strain rates. The yield stress is well described using Eq. (2) over four decades of shifted strain rate. In comparison, the experimental data at any given ΔT is limited to approximately two decades. The insert in Fig. 9 shows the linear relationship between $\log(a_t)$ and T^*.

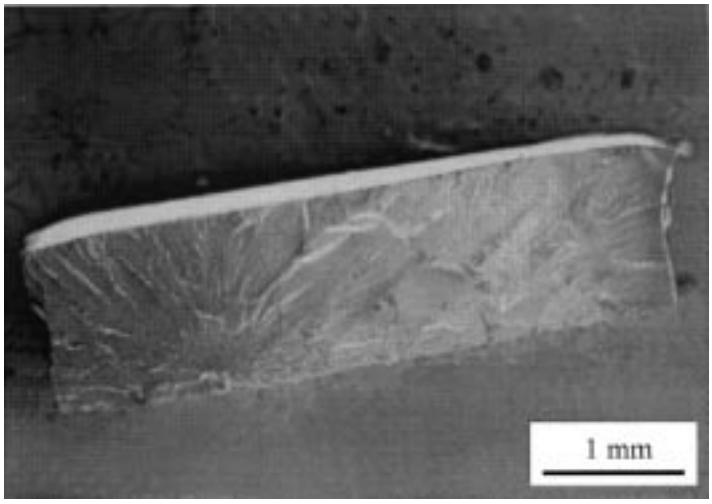

Fig. 6. SEM image of the fracture surface of brittle sample ($\Delta T = -14$°C and $\dot{\epsilon} = 3 \times 10^{-2}\ s^{-1}$).

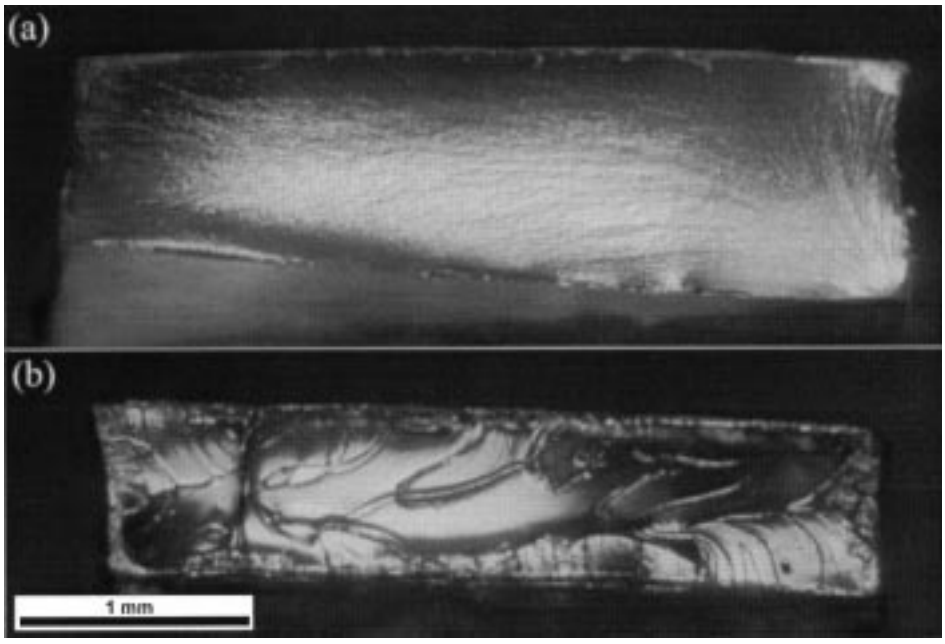

Fig. 7. Optical images of: (a) fracture surface of ductile sample ($\Delta T = +0.5$°C and $\dot{\epsilon} = 0.2\ s^{-1}$); and (b) fracture surface of rubbery sample ($\Delta T = +4$°C and $\dot{\epsilon} = 1 \times 10^{-2}\ s^{-1}$).

3.5. Effect of temperature on yield behaviour

To determine if the effect of moisture content on the tensile properties is equivalent to the effect of temperature, dried PHEE samples were tested at a higher temperature $T_i = 30.5$°C, and corresponding smaller negative ΔT (−6.5°C). This degree of undercooling is the same as for the material conditioned at 30% r.h. At this ΔT, both materials deform in a ductile manner at strain rates between 3.3×10^{-3} and $0.2\ s^{-1}$ and there is a close agreement between their yield stresses, see Fig. 10. From the Eyring model the activation volume for the dried material is $1.3\ nm^3$ which agrees with the v determined previously ($1.5 \pm 0.17\ nm^3$). Therefore, the influence of temperature is analogous to the effect of moisture content on the tensile properties of PHEE.

4. Conclusions

The moisture content has been shown to strongly affect the mechanical properties of PHEE due to changes in the glass transition temperature. As the moisture content increases, there is a reduction in the tensile strength, the yield strength and the modulus but the strain at failure increases. The effect of increasing moisture content is therefore analogous to the effect of increasing temperature.

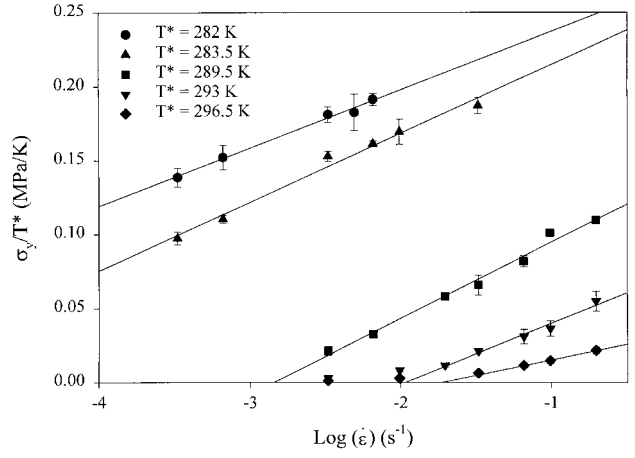

Fig. 8. Ratio of the yield stress, σ_y to T^* versus the logarithm of strain rate fitted to the Eyring equation (Eq. (1)).

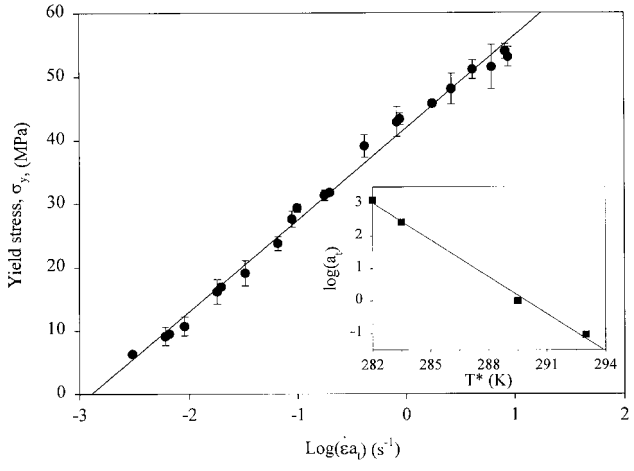

Fig. 9. Master plot of σ_y versus shifted strain rate with a reference $T^* = 289.5$ K. The shift function versus T^* is shown in the insert.

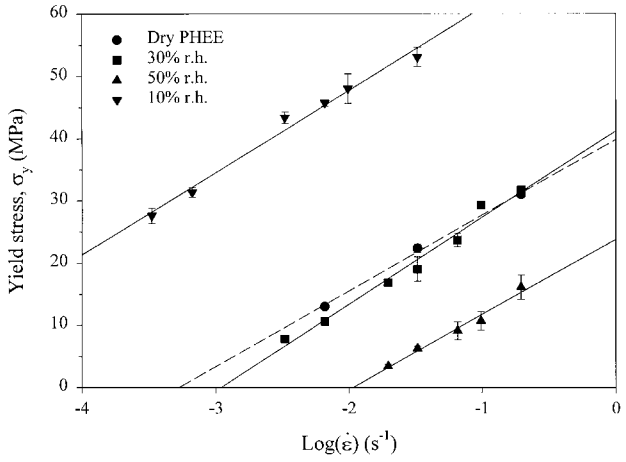

Fig. 10. Yield stress versus log($\dot{\epsilon}$) for: (●) dry PHEE tested at 30.5°C; and (■) PHEE conditioned at 30% r.h. For both materials $\Delta T = -6.5$°C. Also shown is the data for materials conditioned at: (▲) 10% r.h.; and (▼) 50% r.h.

Changes in the T_g or moisture content also alter the mode of failure. As the moisture content increases, PHEE becomes increasingly ductile as shown by the shape of the $\sigma-\epsilon$ curves and the appearance of the fracture surfaces. The variation in yield stress with strain rate and degree of undercooling was well described using the Eyring theory. The ability of this theory to describe the experimental data illustrates that the effect of increasing moisture content is equivalent to an increase in temperature. This was also shown by the agreement between data from tension tests of materials with different moisture content tested at the same ΔT.

Acknowledgements

The authors would like to thank Dr F. Felker for his assistance with the optical microscopy, Dr A. Thompson for scanning electron microscopy and J. Lasanen for her help with sample preparation. This research was conducted under Cooperative Research and Development Agreement 58-3K95-8-633 between ARS and Biotechnology Research Development Corporation.

References

[1] Amass W, Allan A, Tighe B. Polym Int 1998;47:89–144.
[2] Holland SJ, Tighe BJ. Advances in pharmaceutical sciences, vol. 6. San Diego: Academic, 1992. Chap. 4.
[3] Graf A. Eighth Annual Meeting of Bio/Environmentally Degradable Polymer Society, New Orleans, LA, 1999. p. 4.
[4] Willett JL. J Appl Polym Sci 1994;54:1685–95.
[5] Willett JL, St Lawrence S, Doane WM, Mang MN, White JE. Submitted for publication.
[6] St. Lawrence S, Willett JL, Carriere CJ. Proceedings, SPE-ANTEC 2000 — 58th Technical Conference. p. 3640–4.
[7] Walia PS, Lawton JW, Shogren RL, Felker FC. Polymer 1999;41:8083–93.
[8] Wiedmann W, Strobel E. Starch 1991;43:138–45.
[9] Fritz HG, Stuttgart BW. Starch 1993;45:314–22.
[10] George ER, Sullivan TM, Park EH. Polym Engng Sci 1994;34:17–23.
[11] Vaidya UR, Bhattacharya M. J Appl Polym Sci 1994;52:617–28.
[12] Schroeter J, Hobelsberger M. Starch 1992;44:247–52.
[13] Shen J, Chen CC, Sauer JA. Polymer 1985;26:511.
[14] Emri I, Pavsek V. Mater Forum 1992;16:123–31.
[15] Govaert LE, de Vries PJ, Fennis PJ, Nijenhuis WF, Keustermans JP. Polymer 1999;41:1959–62.
[16] Morgan RJ, O'Neal JE, Fanter DL. J Mater Sci 1980;15:751–64.
[17] Mostovoy S, Ripling EJ. J Appl Polym Sci 1971;15:641–59.
[18] Ferry JD. Viscoelastic properties of polymers. 3rd ed. New York: Wiley, 1980. Chap. 11.
[19] Mang MW, White JE, Kram SL, Rick DL, Bailey RE, Swanson PE. Polym Mater Sci Engng 1997;76:412–3.
[20] Mang MW, White JE, Haag AP, Kram SL, Brown CN. Polym Prepr 1995;36:180–1.
[21] Ciao X. Unpublished data.
[22] Andrews EH. Fracture in polymers. New York: Elsevier, 1986. Chap. 2.
[23] Sperling LH. Introduction to physical polymer science. New York: Wiley, 1992. Chap. 8.
[24] G'Sell C, Hiver JM, Dahoun A, Souahi A. J Mater Sci 1992;27:5031–9.
[25] Ishai O. Polym Engng Sci 1969;9:131–40.
[26] Cantwell WJ, Roulin-Moloney AC, Kaiser T. J Mater Sci 1988;23:1615–31.
[27] Crist B. In: Haward RN, Young RJ, editors. The physics of glassy polymers, 2nd ed. London: Chapman & Hall, 1997. Chap. 4.
[28] McCrum NG, Buckley CP, Bucknall CB. Principles of polymer engineering. Oxford: Oxford University Press. Chap. 5.
[29] Ward IM, Hadley DW. An introduction to the mechanical properties of solid polymers. Chichester: Wiley, 1993. Chap. 11.
[30] Moehlenpah AE, Ishai O, diBenedetto AT. J Appl Polym Sci 1969;13:1231–45.